

**Synthesis and Characterization of
Organolanthanidocene(III) (Ln = La, Ce, Pr, Nd)
Complexes Containing the 1,4-Cyclohexa-2,5-dienyl
Ligand (Benzene 1,4-Dianion): Structures of
[K([18]-crown-6)][Ln{ η^5 -C₅H₃(SiMe₃)₂-1,3}₂(C₆H₆)]
[Cp'' = η^5 -C₅H₃(SiMe₃)₂-1,3; Ln = La, Ce, Nd]**

M. Cristina Cassani,[†] Yurii K. Gun'ko,[†] Peter B. Hitchcock,[†]
Michael F. Lappert,^{*,†} and Franco Laschi[‡]

*The Chemistry Laboratory, University of Sussex, Brighton, BN1 9QJ, U.K., and Dipartimento
di Chimica, Università di Siena, Pian dei Mantellini 44, I-52100 Siena, Italy*

Received July 12, 1999

The new tricyclopentadienyllanthanoid metal(III) complexes [LnCp''₃] are obtained in good yields from the appropriate anhydrous metal(III) triflate or chloride and 3/2 MgCp''₂ or 3 KCp'' in tetrahydrofuran at ambient temperature [Cp'' = η^5 -C₅H₃(SiMe₃)₂-1,3 and Ln = La (**1**) or Pr (**3**)]. Treatment of the appropriate compound **1** or **3**, or [CeCp''₃] (**2**) or [NdCp''₃] (**4**), with 2 equiv of each ([18]-crown-6) and potassium in benzene at ambient temperature affords the red or red-brown (**7**) crystalline salts [K([18]-crown-6)][Ln{ η^5 -C₅H₃(SiMe₃)₂-1,3}₂(C₆H₆)] [Ln = La (**5**), Ce (**6**), Pr (**7**), Nd (**8**)], with [K([18]-crown-6)][Cp''] as a coproduct. Each of **5–8** is soluble in hot benzene, which allowed the ¹H NMR spectra to be recorded. The salt **5** is diamagnetic, consistent with its containing a lanthanate(III) anion. For **6–8**, the ¹H NMR spectral signals of the ([18]-crown-6) moiety are only slightly paramagnetically shifted. Hydrolysis of **5** (or **6–8**) yields cyclohexa-1,4-diene. The molecular structures of the isomorphous salts **5**, **6**, and **8** reveal that each comprises a tight ion pair, a C₆H₆ ligand bridging the K and Ln atoms. The potassium atom has close contacts to the six crown ether oxygen atoms and the centroids of the 2,3- and 5,6-carbon atoms of the C₆H₆ ligand. The latter is boat-shaped, the shortest C–Ln distances being those to the 1- and 4-carbon atoms; the endocyclic bond angles at the 1- and 4-carbon atoms are narrower (110.65 ± 1.15°) than those at the other four (122.4 ± 1.2°), while the four C–C bonds to the 1- and 4-carbon atoms are longer (1.46 ± 0.02 Å) than the remaining two (1.350 ± 0.013 Å). The reaction of [LaCp''₃] (**1**) with K and ([18]-crown-6) in benzene, monitored by EPR spectroscopy, reveals the presence of at least four La(II) paramagnetic intermediate species prior to formation of **5**.

Introduction

A continuing quest in our recent research on 4f (Ln) organometallic chemistry is to extend the boundaries of subvalent organometallic Ln compounds beyond the realm of the well-established Sm(II) (4f⁶), Eu(II) (4f⁷), Yb(II) (4f¹⁴), and Ln(0) compounds, many of the Ln(II) complexes being useful one-electron reducing agents.¹ The X-ray structure of [TmI₂(DME)₃] has been published,² and some data are available for a Ce(II)³ and a Nd(II)⁴ complex. Our focus is on tri(cyclopentadienyl)-

metal(III) compounds such as [LnCp''₃] and their reactions with alkali metals [Cp'' = η^5 -C₅H₃(SiMe₃)₂-1,3 and Ln = La (**1**), Ce (**2**), Pr (**3**), or Nd (**4**)]. It is increasingly evident that the nature of the product varies with the reaction medium and the choice of the cyclopentadienyl ligand.

Previously we had shown that the electrochemical reduction of [LaCp''₃] (**1**) in tetrahydrofuran (THF) at a vitreous carbon electrode was reversible, $E_{1/2}$ (La³⁺ ⇌ La²⁺) = -2.8 V relative to the Fc⁺-Fc couple, ferrocene (Fc) being the internal standard,⁵ whereas for [LaCp''₃] $E_{1/2}$ = -3.1 V [Cp'' = η^5 -C₅H₃(CMe₃)₂-1,3]. Furthermore (Scheme 1), we demonstrated that (i) treatment of [LnCp''₃] [Ln = La (**1**),⁵ Ce (**2**),⁶ or Nd (**4**)⁶] with a potassium mirror at ambient temperature induced the

* Corresponding author: School of Chemistry, Physics and Environmental Sciences, University of Sussex, Brighton BN1 9QJ.

[†] University of Sussex.

[‡] Università di Siena.

(1) Edlmann, F. T. In *Comprehensive Organometallic Chemistry*, 2nd ed.; Abel, E. W., Stone, F. G. A., Wilkinson, G., Eds.; Pergamon: Oxford, U.K., 1995; Vol. 4 (Lappert, M. F., Ed.), Chapter 2.

(2) Bochkarev, M. N.; Fedushkin, I.; Fagin, A. A.; Petrovskaya, T. V.; Ziller, J. W.; Broomhall-Dillard, R. N. R.; Evans, W. J. *Angew. Chem., Int. Ed. Engl.* **1997**, *36*, 133.

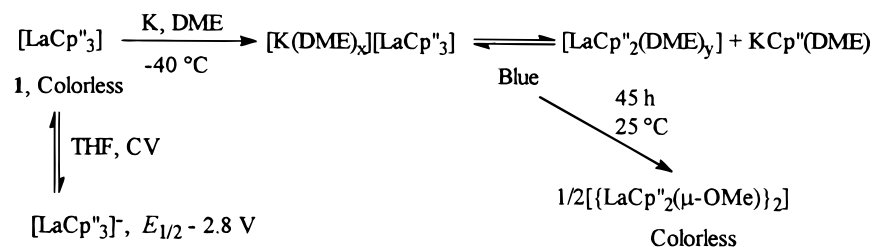
(3) Greco, A.; Cesca, S.; Bertolini, G. *J. Organomet. Chem.* **1976**, *113*, 321.

(4) Wedler, M.; Recknagel, A.; Edlmann, F. T. *J. Organomet. Chem.* **1990**, *395*, C26.

(5) Cassani, M. C.; Lappert, M. F.; Laschi, F. *Chem. Commun.* **1997**, 1563.

(6) Gun'ko, Yu. K.; Hitchcock, P. B.; Lappert, M. F. *J. Organomet. Chem.* **1995**, *499*, 213.

Scheme 1



facile C–O cleavage of 1,2-dimethoxyethane (DME), yielding $[\{\text{LnCp}''_2(\mu\text{-OMe})_2\}]_2$; and (ii) in the $[\text{LaCp}''_3]\text{--K--DME}$ experiment, La(II) species were identified (EPR spectroscopy; ^{139}La , $I = 7/2$) as intermediates.⁵

In two preliminary communications, we reported that upon changing the ether donor from DME to ([18]-crown-6) and using benzene as a reaction medium in the $\text{K--}[\text{LnCp}''_3]$ ($\text{Ln} = \text{La}$ or Ce)^{7,8} or the $\text{K--}[\text{LaCp}''_3]$ ⁷ system C–O fission was not observed. Moreover, these reactions were sensitive to stoichiometry.

From $[\text{LaCp}''_3]$ and ca. 1.5 equiv of potassium, dark green crystals of $[\text{K}(\text{[18]-crown-6})(\eta^2\text{-C}_6\text{H}_6)_2][\{\text{LaCp}''_2(\mu\text{-C}_6\text{H}_6)\}]$ were isolated and structurally authenticated.⁷ The centrosymmetric anion was formulated as comprising two $\text{La}^{\text{II}}\text{Cp}''_2$ moieties bridged by a planar η^6 -benzenide monoanion $[\text{C}_6\text{H}_6]^-$; an alternative of two $\text{La}^{\text{III}}\text{Cp}''_2$ moieties bridged by an $[\eta^6\text{-C}_6\text{H}_6]^{3-}$ ligand was judged to be less plausible.⁷ In the corresponding $[\text{LaCp}''_3]$ experiment, a dark green compound, probably of similar structure, was isolated but not then X-ray-characterized,⁷ although this has since been established,⁹ as will be reported in a full paper.

Employing an excess of potassium, $[\text{LnCp}''_3]$ ($\text{Ln} = \text{La}$ (**1**) or Ce (**2**)) yielded red crystals of $[\text{K}(\text{[18]-crown-6})][\text{LnCp}''_2(\text{C}_6\text{H}_6)]$ ($\text{Ln} = \text{La}$ (**5**) or Ce (**6**)).⁸ The remarkable anions were formulated as $[\text{Ln}^{\text{III}}\text{Cp}''_2(\eta^2\text{-C}_6\text{H}_6)]^-$, containing the boat-shaped 1,4-cyclohexa-2,5-dienyl ligand, i.e., the η^2 -benzenide dianion $[\text{C}_6\text{H}_6]^{2-}$, as established by X-ray crystallography, by the diamagnetism of this $\text{La}(\text{f}^0\text{d}^0)$ complex, and by hydrolysis to give cyclohexa-1,4-diene. In this paper we provide full details and describe extensions of the study to the praseodymium (**7**) and neodymium (**8**) analogues; furthermore, we report on paramagnetic La(II) intermediates, detected by monitoring by EPR spectroscopy the conversion of the diamagnetic $[\text{LaCp}''_3]$ (**1**) into the diamagnetic $[\text{K}(\text{[18]-crown-6})][\text{LaCp}''_2(\text{C}_6\text{H}_6)]$ (**5**).

Experimental Section

Materials and Procedures. All manipulations were carried out under vacuum or argon by Schlenk techniques. Solvents were dried and distilled over sodium–potassium alloy under argon prior to use and then condensed into a reaction flask under vacuum shortly before use. The $[\text{Ln}\{\eta^5\text{-C}_5\text{H}_3\text{-}(\text{SiMe}_3)_2\text{-1,3}\}_3]$ ($\text{Ln} = \text{Ce}$ (**2**) or Nd (**3**)) complexes were prepared by known procedures.^{6,10} KCp'' , MgCp''_2 and $\text{La}(\text{OSO}_2\text{CF}_3)_3$ were prepared as described previously. ([18]-Crown-6) (Acros

Chemicals) was crystallized from acetonitrile; the adduct was set aside for 1 day under vacuum and recrystallized from hexane.

Microanalyses were carried out by Medac Ltd. (Brunel University). The NMR spectra were recorded using the following Bruker instruments: AC-P 250 (^1H , 250.1; ^{13}C , 62.9; ^{29}Si 49.7 MHz), DPX 300 (^1H , 300.1; ^{13}C 75.5 MHz), and AMX 500 (^1H , 500.1; ^{13}C , 125.7 MHz) and referenced internally to residual solvent resonances (data in δ) in the case of ^1H and ^{13}C spectra; ^{29}Si spectra were referenced externally to SiMe_4 . Unless otherwise stated, all NMR spectra other than ^1H were proton-decoupled. Deuterated benzene and THF were dried over Na/K alloy and distilled prior to use.

Electron impact mass spectra were taken from solid samples using a Kratos MS 80 RF instrument; GC/MS analysis was performed on a HP 5995 gas chromatography mass spectrometer. Melting points were taken in sealed capillaries and are uncorrected.

X-band electron paramagnetic resonance (EPR) spectra were recorded with a ER 200 D-SRC Bruker spectrometer operating at $\nu = 9.44$ GHz using a HS Bruker rectangular cavity. The control of the operational frequency ν was obtained with a Hewlett-Packard X5-32B wavemeter, and the applied magnetic field was calibrated with a DPPH sample (diphenylpicrylhydrazyl free radical) as a suitable field marker. The control of the temperature was obtained with a Bruker ER 4411 VT device ($T = \pm 1$ K). The experimental g values are referred to the g_{DPPH} value ($g_{\text{DPPH}} = 2.0036$) used as external standard reference. The errors affecting the g , A_i , and ΔH_i values are $\pm 5 \times 10^{-3}$ G, $\pm 2 \times 10^{-1}$ G, and ± 2 G, respectively. The samples were prepared according to the following general procedure: potassium (mirror), freshly distilled benzene, and the complex $[\text{LaCp}''_3]$ (**1**) were introduced into a Schlenk tube with a quartz tube connected on one side. After stirring for 30 min, ([18]-crown-6) was added as a solid at room temperature, and in few minutes the yellow solution turned dark violet. Part of the reaction mixture was transferred to the connected quartz tube and analyzed via EPR spectroscopy under the described experimental conditions.

Synthesis of $[\text{LaCp}''_3]$ (1**).** (a) To a mixture of anhydrous $\text{La}(\text{OSO}_2\text{CF}_3)_3$ (5.0 g, 8.6 mmol) and MgCp''_2 (5.77 g, 13.0 mmol) was added THF (50 mL). The mixture was stirred for 24 h at room temperature, gradually producing a white fluffy precipitate. After filtration the volatiles were removed from the filtrate under reduced pressure and the solid was washed with hexane (3×20 mL). The combined washings were concentrated to a small volume and cooled at -22 $^\circ\text{C}$, yielding colorless crystals of **1** (two crops, 4.7 g, 71%). ^1H NMR (C_6D_6): δ 6.88 (t, 3H, $^4J = 1.9$ Hz), 6.81 (d, 6H, $^4J = 1.9$ Hz), 0.32 (s, 54H). ^{13}C NMR (C_6D_6): δ 131.6 (2CH) 130.4 (C_{quat}) 126.0 (1CH) 0.89 (SiMe_3). ^{29}Si (C_6D_6): δ -10.2 . Anal. Calcd for $\text{C}_{33}\text{H}_{63}\text{-LaSi}_6$: C, 51.7; H, 8.28. Found: C, 50.8; H, 8.22. EI-MS: m/z 751 ($[\text{M} - \text{Me}]^+$, 9), 693 ($[\text{M} - \text{SiMe}_3]^+$, 35), 557 ($[\text{LaCp}''_2]^+$, 75), 73 ($[\text{SiMe}_3]^+$, 100). IR (Nujol, $\nu_{\text{max}}/\text{cm}^{-1}$): 3075m, 3051m, 1436s, 1403m, 1319m, 1246vs, 1211m, 1202m, 1079vs, 920vs, 835vs br, 775s, 751s, 689s, 641s, 621s. Mp: 220 $^\circ\text{C}$.

(b) A solution of KCp'' (5.6 g, 2.58 mmol) in tetrahydrofuran (100 mL) was added to a stirred suspension of LaCl_3 (1.85 g, 7.53 mmol) in tetrahydrofuran (100 mL). The mixture was

(7) Cassani, M. C.; Duncalf, D. J.; Lappert, M. F. *J. Am. Chem. Soc.* **1998**, *120*, 12958.

(8) Cassani, M. C.; Gun'ko, Yu. K.; Hitchcock, P. B.; Lappert, M. F. *Chem. Commun.* **1996**, 1987.

(9) Gun'ko, Yu. K.; Hitchcock, P. B.; Lappert, M. F. Unpublished work.

(10) Sofield, C. D.; Andersen, R. A. *J. Organomet. Chem.* **1995**, *501*, 271.

Table 1. Crystal Data and Structure Refinement for 5, 6, and 8

	5	6	8
formula	C ₄₀ H ₇₂ KLaO ₆ Si ₄ ·0.5C ₆ H ₆	C ₄₀ H ₇₂ CeKO ₆ Si ₄ ·0.5C ₆ H ₆	C ₄₀ H ₇₂ KNdO ₆ Si ₄ ·0.5C ₆ H ₆
<i>M</i>	978.4	979.6	983.7
cryst syst	monoclinic	monoclinic	monoclinic
space group	<i>P</i> 2 ₁ / <i>n</i> (No. 14)	<i>P</i> 2 ₁ / <i>n</i> (No. 14)	<i>P</i> 2 ₁ / <i>n</i> (No. 14)
<i>a</i> , <i>b</i> , <i>c</i> (Å)	14.236(4), 16.580(5), 22.567(9)	14.185(10), 16.544(3), 22.592(7)	14.140(4), 16.500(7), 22.575(10)
β (deg)	106.26(3)	106.09(4)	105.97(3)
<i>U</i> (Å ³), <i>Z</i> , <i>D</i> _c (g cm ⁻³)	5114(3), 4, 1.27	5094(4), 4, 1.28	5064(3), 0.4, 1.29
<i>T</i> (K)	173	173	173
μ(Mo Kα) (mm ⁻¹)	1.05	1.11	1.24
cryst size (mm)	0.35 × 0.3 × 0.2	0.4 × 0.4 × 0.3	0.4 × 0.4 × 0.35
total no. of unique reflns	12311 (2° < θ < 28°)	8936 (2° < θ < 25°)	7011 (2° < θ < 23°)
no. of reflns with [<i>I</i> > 2σ(<i>I</i>)]	8090	6718	5831
<i>R</i> ₁ , <i>wR</i> ₂ ^a	0.058, 0.145	0.044, 0.095	0.037, 0.095

^a *R*₁ = Σ(|*F*_o - |*F*_c||)/Σ(|*F*_o|). *wR*₂ = [Σ*w*(|*F*_o|² - |*F*_c|²)/Σ*w*(|*F*_o|²)^{1/2}] for all data.

stirred for 24 h at room temperature. The tetrahydrofuran was removed in vacuo, and toluene (100 mL) was added to the residue. The mixture was heated under reflux for 24 h, giving a pale yellow-brown suspension. The toluene was removed in vacuo, and the resultant solid residue was extracted into hexane (150 mL). The extract was filtered and the filtrate concentrated to ca. 10 mL. Cooling to -22 °C afforded colorless crystals of compound **1** (3.75 g, 65%).

Synthesis of [PrCp''₃] (3). The reaction of KCp'' (1.90 g, 7.66 mmol) and PrCl₃ (0.63 g, 2.55 mmol), using the procedure (b) described for **1**, afforded bright yellow crystals of compound **3** (1.5 g, 77%). Anal. Calcd for C₃₃H₆₃Si₆Pr: C, 51.6; H, 8.20. Found: C, 51.6; H, 8.26. ¹H NMR (300 MHz, C₆D₆, 293 K): δ 59.54 (br, 1H, Cp ring), 32.76 (br, 6H, Cp ring), -12.44 (s, 54H, SiMe₃). MS: *m/z* 768 ([M]⁺, 0.08); 695 ([M - SiMe₃]⁺, 6); 559 ([PrCp''₂]⁺, 90); 209 ([Cp^R]⁺, 7); 73 ([SiMe₃]⁺, 100).

Synthesis of [K([18]-crown-6)][La{η⁵-C₅H₃(SiMe₃)₂-1,3}-C₆H₆] (5). A solution of [LaCp''₃] (**1**) (0.73 g, 0.95 mmol) in benzene (70 mL) was added to a mirror of metallic potassium (0.075 g, 1.92 mmol). Then ([18]-crown-6) (0.50 g, 1.92 mmol) was added, and the mixture was stirred for 5 h until all the potassium had dissolved. The deep red suspension was filtered, using a thoroughly dried glass microfiber, and the filtrate was concentrated in vacuo to ca. 20 mL. Deep red crystals of **5** were gradually deposited. Cooling to +4 °C afforded an additional crop of crystals of **5** (total yield, 0.49 g, 55%). Anal. Calcd for C₄₀H₇₂KLaO₆Si₄: C, 51.2; H, 7.68. Found: C, 51.6; H, 8.06. ¹H NMR (C₆D₆, 333 K): δ 7.24 (d, 4H, ⁴*J* 1.9 Hz, Cp ring), 5.14 (t, 2H, ⁴*J* 2.0 Hz, Cp ring), 3.04 (s, 24H, [18]-crown-6), 0.46 (s, 36H, SiMe₃). UV-vis (benzene, λ_{max}/nm, 293 K): 486, 338 (sh) 279. IR (Nujol, ν_{max}/cm⁻¹): 1554w, 1351m, 1242m, 1113vs, 1077s, 963m, 831s.

Further concentration of the rest of the mother solution and cooling to +4 °C afforded colorless crystals of [K([18]-crown-6)][Cp''] (0.39 g, 81%). Anal. Calcd for C₂₃H₄₅KO₆Si₂: C, 53.9; H, 7.79. Found: C, 53.6; H, 7.66. ¹H NMR (C₆D₆, 333 K): δ 6.73 (d, 2H, Cp ring); 6.57 (t, 4H, Cp ring), 3.14 (s, 24H, [18]-crown-6), 0.53 (s, 36H, SiMe₃).

Synthesis of [K([18]-crown-6)][Ce{η⁵-C₅H₃(SiMe₃)₂-1,3}-C₆H₆] (6). The reaction of [CeCp''₃] (**2**) (0.85 g, 1.11 mmol), potassium (0.086, 2.2 mmol), and ([18]-crown-6) (0.58 g, 2.2 mmol), using the procedure described for **5**, afforded dark red crystals of complex **6** (0.52 g, 50%). Anal. Calcd for C₄₀H₇₂-KCeO₆Si₄: C, 51.1; H, 7.67. Found: C, 51.0; H, 7.56. ¹H NMR (C₆D₆, 323 K): δ 16.80 (br, 4H, Cp ring), 2.92 (s, 24H, [18]-crown-6), -5.34 (s, 36H, SiMe₃), -49.29 (br, 2H, Cp ring). UV-vis (benzene, λ_{max}/nm, 293 K): 461, 340 (sh), 278. The IR spectrum (Nujol) was identical to that for **5**. Colorless crystals of [K([18]-crown-6)][Cp''] (0.44 g, 78%) were obtained, using the procedure described in the previous experiment. Anal. Calcd for C₂₃H₄₅KO₆Si₂: C, 53.9; H, 7.79. Found: C, 54.0; H, 7.85. The NMR spectrum was identical to that in the previous experiment.

Synthesis of [K([18]-crown-6)][Pr{η⁵-C₅H₃(SiMe₃)₂-1,3}-C₆H₆] (7). The reaction of [PrCp''₃] (**3**) (0.68 g, 0.885 mmol),

potassium (0.069, 1.77 mmol), and ([18]-crown-6) (0.47 g, 1.77 mmol), using the procedure described for **5**, afforded dark red-brown crystals of complex **7** (0.49 g, 59%). Anal. Calcd for C₄₀H₇₂KPrO₆Si₄: C, 51.1; H, 7.66. Found: C, 51.9; H, 7.81. ¹H NMR (C₆D₆, 323 K): δ 14.70 (br, 4H, Cp ring); 2.69 (s, 24H, [18]-crown-6), -3.68 (s, 36H, SiMe₃), -13.11 (br, 2H, Cp ring). UV-vis (benzene, λ_{max}/nm, 293 K): 443, 358 (sh) 282. The IR spectrum (Nujol) was identical to that for **5**. Colorless crystals of [K([18]-crown-6)][Cp''] (0.38 g, 85%) were obtained, using the procedure described above. Anal. Calcd for C₂₃H₄₅KO₆Si₂: C, 53.9; H, 7.79. Found: C, 54.2; H, 7.83. The NMR spectrum was identical to those reported above.

Synthesis of [K([18]-crown-6)][Nd{η⁵-C₅H₃(SiMe₃)₂-1,3}-C₆H₆] (8). The reaction of [NdCp''₃] (**4**) (0.80 g, 1.04 mmol), potassium (0.081, 2.08 mmol), and ([18]-crown-6) (0.55 g, 2.08 mmol), using the procedure described for **5**, afforded dark red crystals of complex **8** (0.60 g, 61%). Anal. Calcd for C₄₀H₇₂KNdO₆Si₄: C, 50.9; H, 7.63. Found: C, 51.0; H, 7.67. ¹H NMR (C₆D₆, 323 K): δ 8.71 (br, 4H, Cp ring), 3.72 (s, 24H, [18]-crown-6), -3.05 (br, 2H, Cp ring), -3.97 (s, 36H, SiMe₃). UV-vis (benzene, λ_{max}/nm, 293 K): 446 (br), 340 (sh) 281. The IR spectrum (Nujol) was identical to that for **5**. Colorless crystals of K([18]-crown-6)][Cp''] (0.44 g, 78%) were obtained, using the procedure described above. Anal. Calcd for C₂₃H₄₅-KO₆Si₂: C, 53.9; H, 7.79. Found: C, 54.3; H, 7.84. The NMR spectrum was identical to those reported above.

Crystallographic Structure Determination of Complexes. Single crystals of each of the salts **5**, **6**, and **8** were obtained by concentrating the filtered solutions of the products at room temperature. Data were measured on an Enraf-Nonius CAD4 diffractometer using monochromated Mo Kα radiation. A crystal of the salt **5**, **6**, or **8** was coated in oil and cooled. Corrections for absorption were made using ψ-scan measurements.

Structure solutions were made using SHELXS-86.^{11a} Refinement was based on *F*², with H atoms in riding mode, using SHELXL-93.^{11b}

Further details are given in Table 1.

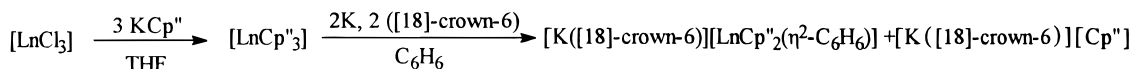
Results and Discussion

Synthesis and Characterization of [K([18]-crown-6)][LnCp''₂(η²-C₆H₆)] 5-8. The starting compounds [LnCp''₃] [Ln = La (**1**), Ce (**2**), Pr (**3**), Nd (**4**)] were prepared in good yield from the appropriate anhydrous lanthanoid metal(III) triflate or chloride and magnesium or potassium cyclopentadienide, according to procedures previously described for **2** and **4**.^{6,10,12} Compounds **1** and **3** were identified by elemental analysis, EI-mass

(11) (a) Sheldrick, G. M. In *Crystallographic Computing 3*; Sheldrick, G. M., Krüger, C., Goddard, R., Eds.; Oxford University Press: Oxford, 1985; pp 175-189. (b) Sheldrick, G. M. *SHELXL-93*, a program for crystal structure refinement; University of Göttingen, 1993.

(12) Al-Juaid, S.; Gun'ko, Yu. K.; Hitchcock, P. B.; Lappert, M. F.; Tian, S. *J. Organomet. Chem.* **1999**, *582*, 143.

Scheme 2



1 Ln = La, colorless, 65 %

2 Ln = Ce, blue, (ref. 7)

3 Ln = Pr, yellow, 77 %

4 Ln = Nd, green (ref. 7)

5 Ln = La, red, 55 %

6 Ln = Ce, red, 50 %

7 Ln = Pr, red-brown, 59 %

8 Ln = Nd, red, 61 %

$[\text{LnCp}''_2]^+$ as base peak and weak $[\text{LnCp}''_3]^+$) and ^1H NMR spectra.

Treatment of the appropriate compound 1–4 with 2 equiv each of a potassium mirror and ([18]-crown-6) in benzene at ambient temperature afforded a dark red solution from which crystals of $[\text{K}(\text{[18-crown-6]})][\text{LnCp}''_2(\eta^2\text{-C}_6\text{H}_6)]$ [Ln = La (5), Ce (6), Pr (7), Nd (8)] were obtained, after filtration, by concentration and cooling. Further concentration and cooling gave the colorless precipitate of $[\text{K}(\text{[18-crown-6]})][\text{Cp}'']$, identified by elemental analysis and ^1H NMR spectroscopy. The syntheses are summarized in Scheme 2.

Complexes 5–8 had a limited solubility in benzene, which enabled them to be readily separated from the more soluble coproduct $[\text{K}(\text{[18-crown-6]})][\text{Cp}'']$. They were characterized by elemental analyses and spectra.

The ^1H NMR spectrum in *hot* C_6D_6 (5, like 6–8, was only sparingly soluble in benzene) was particularly informative for the diamagnetic lanthanum complex 5. Although the analogues 6–8 gave paramagnetically shifted Cp'' signals, assignments were readily made, on the basis of signal intensities. The anionic nature of the Ln environment in 5–8 resulted in the Cp'' signals being shifted to higher frequency compared with those in the appropriate neutral precursor $[\text{LnCp}''_3]$ 1–4. Signals due to the ([18]-crown-6) moiety were only slightly shifted in the paramagnetic complexes 6–8 compared with those in the diamagnetic La analogue 5. The signals of the 1,4-cyclohexa-2,5-dienyl ligand were not detected, attributed to a fast exchange with the heated deuterated benzene solvent. Alternatively, as suggested by a referee, it is possible that 5 is fluxional, 1,2-sigmatropic shifts averaging the benzene signals on an intermediate time scale. We conclude that the ^1H NMR solution spectra for 5–8 are consistent with the structures revealed for the crystalline complexes 5, 6, and 8 (*vide infra*).

The UV–vis spectra in benzene of complexes 5–8 showed a similar pattern of absorption bands: at 463 ± 23 nm, a shoulder at 348 ± 10 nm, and a band at 280 ± 2 nm. These values are similar to those reported previously for a solution of potassium and (perhydrodibenzo-18-crown-6) in benzene (λ_{max} 435 and 300 nm),¹³ or potassium and DME in benzene at 203 K (λ_{max} 435 and 285 nm),¹⁴ which in both cases were attributed to the benzene monoanion. The IR spectrum of each of 5–8 was identical.

Crystals of each of the complexes 5–8 were extremely air-, moisture-, and temperature- (slowly decomposed at >80 °C) sensitive. While sparingly soluble in aromatic

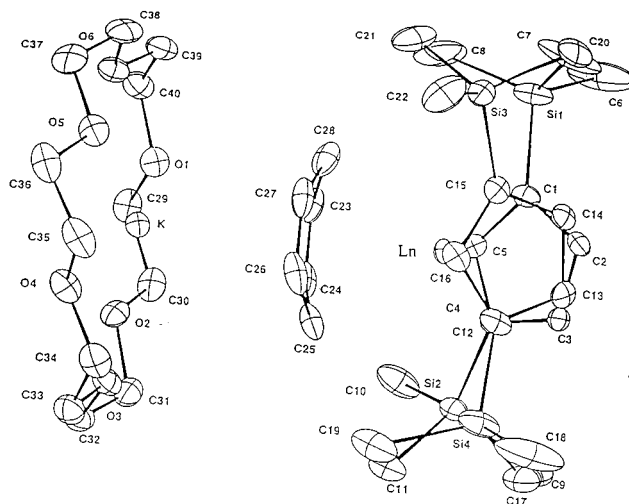


Figure 1. Molecular structure of the isostructural compounds $[\text{K}(\text{[18-crown-6]})][\text{Ln}\{\eta^5\text{-C}_5\text{H}_3(\text{SiMe}_3)_{2-1,3}\}_2(\text{C}_6\text{H}_6)]$ 5, 6, and 8. The example chosen relates to 6 showing 50% probability ellipsoids and the atom-labeling scheme for Ln = Ce.

hydrocarbons at ambient temperature, and insoluble in aliphatic hydrocarbons, they dissolved readily in diethyl ether or THF.

Upon hydrolysis each of the crystalline complexes 5–8 in aqueous diethyl ether yielded cyclohexa-1,4-diene and a smaller portion of benzene, as established by GC–MS.

X-ray Crystal Structures of 5, 6, and 8. The crystalline complexes 5, 6, and 8 are isostructural. Alternative views of the molecular structure and the atom-numbering scheme are shown in Figures 2 and 3. Selected bond distances and angles are listed in Tables 2 and 3.

Each of the crystalline molecules 5, 6, and 8 consists of a tight ion pair, the C_6H_6 ligand separating the potassium and lanthanoid metal atoms. There is also a noncoordinating benzene solvate molecule lying on an inversion center.

The geometric parameters for the cation $[\text{K}(\text{[18-crown-6]})]^+$ are similar for each of 5, 6, and 8, the K–O distances ranging from 2.769(3) to 2.876(3) Å. This may be compared with the 2.747(4)–2.818(4) Å in $[\text{K}(\text{[18-crown-6]})][\text{Fe}_4\{\text{Au}(\text{PET}_3)\}_2(\text{CO})_{13}\cdot\text{CH}_2\text{Cl}_2]$ (the six crown oxygen atoms being equatorial, with two isocarbonyl oxygen atoms in axial positions¹⁵) or $[\text{K}(\text{[18-crown-6]})][\text{Rh}(\text{CO})_2\{\text{P}(\text{OEt})_3\}_2\text{-trans}]$, in which the K–O environment is completed by one isocarbonyl and one phosphite oxygen atom.¹⁶ As in these two complexes, and also in 5, 6, and 8, the potassium atom environment has two close noncrown contacts: involving the 2,3- and 5,6-

(13) Gardner, C. L. *J. Chem. Phys.* **1966**, *45*, 572.

(14) Kaempf, B.; Raynal, S.; Collet, A.; Schué, F.; Boileau, S.; Lehn, J.-M. *Angew. Chem., Int. Ed. Engl.* **1974**, *13*, 611.

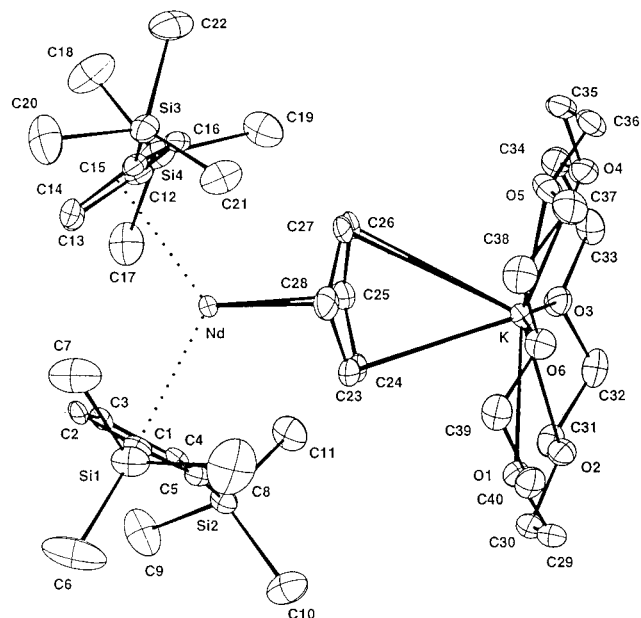


Figure 2. Alternative view of $[K([18]\text{-crown-6})][Nd\{\eta^5\text{-}C_5H_3(SiMe_3)_2\text{-}1,3\}_2(C_6H_6)]$ **8**.

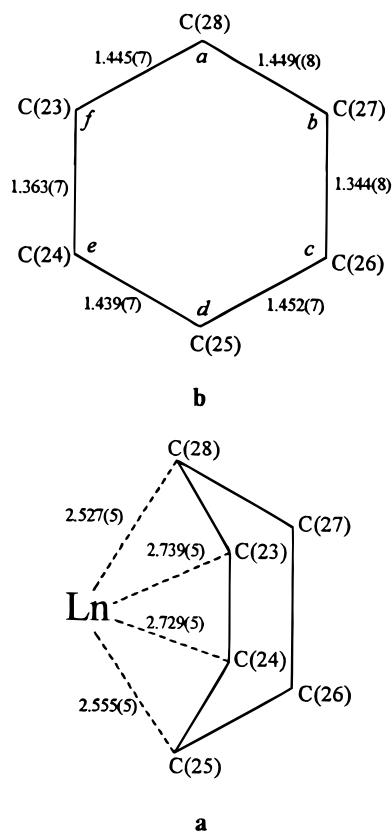


Figure 3. Schematic representation of the $Ln(C_6H_6)$ moiety, showing selected bond lengths (Å) and angles a – f (deg) for the bridging C_6H_6 ligand (b), and its binding to the Ln atom (a), illustrated for the case of $Ln = Nd$ [$Nd-C(27)$ 2.761(5), $Nd-C(26)$ 2.763(5) Å; a 111.8(5)°, b 122.9(5)°, c 121.5(5)°, d 111.7(5)°, e 122.7(5)°, f 121.2(5)°].

carbons [C(23), C(24) and C(26), C(27) in Figure 2] of the bridging C_6H_6 ligand which range from 3.046(5) to 3.395(5) Å, the 1,4-[C(25) and C(28)] carbons being more remote. These $K \cdots C$ contacts may be compared with (i) the 3.270(10) and 3.495(11) Å in $[K([18]\text{-crown-6})(\eta^2\text{-}$

Table 2. Selected Bond Lengths (Å) for **5**, **6**, and **8**^a

bond	5	6	8
Ln–M(1)	2.624(6)	2.604	2.570
Ln–M(2)	2.628(6)	2.597	2.557
Ln–C ₆ H ₆ (centr)	2.427(6)	2.328	2.292
Ln–C(23)	2.805(6)	2.774(5)	2.739(5)
Ln–C(24)	2.785(6)	2.767(5)	2.729(5)
Ln–C(25)	2.617(6)	2.588(5)	2.555(5)
Ln–C(26)	2.794(6)	2.784(5)	2.763(5)
Ln–C(27)	2.811(6)	2.787(5)	2.761(5)
Ln–C(28)	2.652(6)	2.612(5)	2.572(5)
C(23)–C(24)	1.358(10)	1.350(8)	1.363(7)
C(23)–C(25)	1.471(9)	1.463(7)	1.445(7)
C(24)–C(25)	1.456(10)	1.442(8)	1.439(7)
C(25)–C(26)	1.480(9)	1.464(7)	1.452(7)
C(26)–C(27)	1.337(11)	1.352(9)	1.344(8)
C(27)–C(28)	1.447(10)	1.443(8)	1.449(8)
K–O(1)	2.859(4)	2.867(4)	2.876(3)
K–O(2)	2.861(4)	2.856(4)	2.851(3)
K–O(3)	2.820(4)	2.817(3)	2.814(3)
K–O(4)	2.833(4)	2.823(4)	2.811(3)
K–O(5)	2.783(4)	2.776(4)	2.769(3)
K–O(6)	2.867(5)	2.869(4)	2.875(3)
K–C(23)	3.145(7)	3.087(5)	3.046(5)
K–C(24)	3.097(6)	3.094(5)	3.107(5)
K–C(26)	3.275(7)	3.336(6)	3.395(5)
K–C(27)	3.324(6)	3.329(5)	3.328(5)

^a M(1) and M(2) are the centroids of the C(1)–C(5) and C(12)–C(16), cyclopentadienyl rings, respectively.

Table 3. Selected Bond Angles (deg) for **5**, **6**, and **8**^a

angle	5	6	8
M(1)–Ln–M(2)	116.7	116.9	117.1
C ₆ H ₆ (centr)–Ln–M(1)	120.5	120.6	120.5
C ₆ H ₆ (centr)–Ln–M(2)	122.8	122.6	122.3
Ln–C ₆ H ₆ (centr)–K	174.2	173.4	171.3
M(1)–Ln–C(25)	114.7	114.9	114.5
M(2)–Ln–C(25)	116.0	116.1	115.9
M(1)–Ln–C(28)	114.7	115.0	115.1
M(2)–Ln–C(28)	117.8	117.0	116.6
C(25)–Ln–C(28)	67.9	67.8	68.6
C(24)–C(23)–C(28)	121.9(7)	121.9(5)	121.2(5)
C(23)–C(24)–C(25)	123.6(6)	122.7(5)	122.7(5)
C(24)–C(25)–C(26)	109.5(7)	111.6(5)	111.7(5)
C(27)–C(26)–C(25)	123.5(7)	121.7(5)	121.5(5)
C(26)–C(27)–C(28)	123.0(6)	122.7(5)	122.9(5)
C(27)–C(28)–C(23)	111.2(7)	111.7(5)	111.8(5)
C(28)C(23)C(24)C(25)/ C(28)C(27)C(26)C(25)	23.6	23.5	24.7

^a M(1) and M(2) are the centroids of the C(1)–C(5) and C(12)–C(16) cyclopentadienyl rings, respectively.

$C_6H_6)_2][[LaCp^{tt}_2]_2(\mu\text{-}\eta^6\text{-}C_6H_6)]$, having K–O bond lengths of 2.748(5)–2.847(4) Å;⁷ (ii) the 3.53(3) Å in $[K([18]\text{-crown-6})(\eta^2\text{-}C_6H_5Me)_2][SmCp''_3]$, having K–O bond lengths of 2.72(2)–2.83(2) Å;¹⁷ or (iii) the 3.28(2)–3.60(2) Å in $K\{Sn(CH_2Bu^t)_3\}(\eta^6\text{-}C_6H_5Me)_3$.¹⁸

The lanthanoid metal environment in each of the $[LnCp''_2(C_6H_6)]^-$ anions **5**, **6**, and **8** may be described as being quasi-12-coordinate, 10 sites being occupied by the two Cp'' ligands and the two remaining by the 1,4-carbons [C(25) and C(28)] of the C_6H_6 ligand. The latter thus adopts a boat conformation, illustrated schematically in Figure 3a. The dihedral angles between the

(15) Horwitz, C. P.; Holt, E. M.; Brock, C. K.; Shriver, D. F. *J. Am. Chem. Soc.* **1985**, *107*, 8136.

(16) Chan, A. S. C.; Shieh, H.-S.; Hill, J. R. *J. Organomet. Chem.* **1985**, *279*, 171.

(17) Gun'ko, Yu. K.; Hitchcock, P. B.; Lappert, M. F. *Chem. Commun.* **1998**, 1843.

(18) Hitchcock, P. B.; Lappert, M. F.; Lawless, G. A.; Royo, B. *J. Chem. Soc., Chem. Commun.* **1993**, 554.

C(28)–C(23)–C(24)–C(25) and C(28)–C(27)–C(26)–C(25) planes, the fold angle of the C₆H₆ ligand, is approximately 24° for each of the three anions. The endocyclic bond angles in the C₆H₆ ligand at C(25) and C(28) are narrower (110.7 ± 1.2°) than those at the remaining four carbon atoms (122.4 ± 1.2°), and the four C–C bonds to C(25) and C(28) are longer (1.46 ± 0.02 Å) than the remaining two (1.35 ± 0.01 Å), illustrated schematically in Figure 3b.

The Ln–C(C₆H₆), like the Ln–C(Cp), bond lengths in each anion of **5**, **6**, or **8** are broadly similar, but show the expected lanthanide contraction: La–C > Ce–C > Nd–C. The Ln–C(25) and Ln–C(28) bonds are ca. 0.18 Å shorter than the other four Ln–C(C₆H₆) bonds, Figure 3a, which lends further support to the notion that the ligated C₆H₆ is the 1,4-cyclohexa-2,5-dienyl ligand.

The diene–diyl nature of some transition metal-coordinated *substituted* arene ligands has been discussed.^{19–21} For instance, in [TaCl₂(OC₆H₃Prⁱ₂-2,6)(C₆Me₆)], (i) the Ta–C bonds to the 1,4-carbon atoms of C₆Me₆ are ca. 0.265 Å shorter than those to the other four carbon bonds, (ii) the endocyclic C–C bonds to the 1,4-carbon atoms are ca. 0.085 Å shorter than the mean of 1.462 Å for the other two, and (iii) the fold angle is 26.8°.¹⁹ Bonding between an arene and a lanthanoid metal has been reviewed.²² Systems related to the present work dealt with lutetium binding to a coordinated naphthalene²³ or anthracene,²⁴ as in [Lu(η⁵-C₅H₅)-(C₁₀H₈)(DME)].²³ The latter was obtained from Lu(η⁵-C₅H₅)Cl₂ + 2 Na(C₁₀H₈) in 1,2-dimethoxyethane and upon hydrolysis yielded a mixture of 1,4- and 1,2-dihydronaphthalenes.

The La–C(C₆H₆) bond lengths to C(25) and C(28) of 2.635 ± 0.018 Å for **5** may be compared with the only published La–C_{aryl} bond distance of 2.548(1) Å in [La(η⁵-C₅H₅)₂{C₆H₃(NMe₂)₂-2,6}].²⁵ In the latter, the La–C(C₅H₅) bond lengths range from 2.785(4) to 2.926(5) Å, whereas the La–C(Cp'') bond distances are 2.898 ± 0.056 in **5**, and 2.835 ± 0.035 Å in [LaCp''₂(NCMe)(DME)][BPh₄]·0.5DME.²⁶ For the cerium complex **6**, the Ce–C(Cp'') bond lengths range from 2.822(5) to 2.909(5) Å, which is similar to the average of 2.83 or 2.87 Å in [CeCp''₃] (**2**) or [CeCp''₃(NCMe)], respectively.²⁷ For the neodymium anion of **8**, there is the opportunity to make comparison with an anionic complex also bearing two Cp'' ligands. Thus, the mean Nd–C(Cp) bond length in **8** of 2.83 Å is only very slightly longer than the average of 2.78 Å in the neodyminate(III) salt [AsPh₄][NdCp''₂Cl₂],²⁸ in which the Cp''–Nd–Cp'' angle of

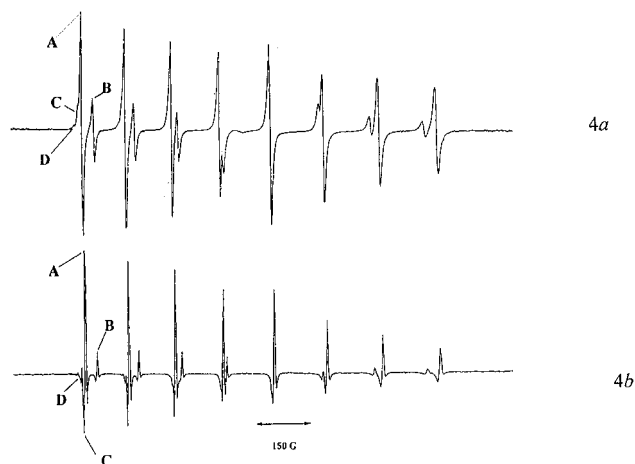


Figure 4. X-Band EPR spectra of the paramagnetic La(II) species A–D in (a) first derivative mode and (b) second derivative mode, $T = 280$ K.

126.3° is slightly wider than the 117.1(1)° in **8**, attributed to the presence of the chelating C₆H₆ ligand in the latter. An alternative view of the coordination environment about the Ln metal atom in the anion **5**, **6**, and **8** is to describe this as distorted tetrahedral, taking the Cp'' ligand centroids and the 1- and 4-carbons of the C₆H₆ ligand as occupying the four coordination sites.

X-Band EPR Spectroscopic Analysis. The reaction of [LaCp''₃] (**1**) with K and ([18]-crown-6) in benzene at room temperature was monitored by EPR spectroscopy. The addition of ([18]-crown-6) to a slightly yellow solution of **1** in benzene, in the presence of a potassium mirror, led to the immediate formation of a paramagnetic, dark violet-blue solution, the EPR spectra of which clearly revealed it to contain at least four paramagnetic lanthanum(II) species.

The line shape analysis of the four sets of signals can be suitably carried out assuming the $S = 1/2$ electron spin Hamiltonian in the general form

$$\mathbf{H} = gH\beta S + IAS + \sum_i I_i A_i S$$

Here, the first term accounts for the Zeeman energy relevant to the interaction of the unpaired electron with the applied magnetic field H , S being the electron spin operator. The second term refers to the A hyperfine interaction between the S electron spin and the I nuclear spin, I being the nuclear spin operator of the most abundant lanthanum isotope (¹³⁹La: 99.91% natural abundance; $\mu = +2.776$, $I = 7/2$). The third term refers to the summation of the A_i superhyperfine interaction between the S electron spin and the I_i nuclear spin of the magnetically active i th nucleus of the different ligand atoms (if any) of the first coordination sphere.

Figure 4 shows the first (Figure 4a) and the second (Figure 4b) derivative EPR spectra of the paramagnetic solution recorded at 280 K, which consisted of four sets of partially superimposed multiplets, each displaying well-resolved metal-in-character signals ($g_{\text{isotropic}} \neq g_{\text{elec}} = 2.0023$).

(28) Lappert, M. F.; Singh, A.; Atwood, J. L.; Hunter, W. E.; Zhang, H.-M. *J. Chem. Soc., Chem. Commun.* **1983**, 69.

(19) Arney, D. J.; Wexler, P. A.; Wigley, D. E. *Organometallics* **1990**, 9, 1282, and references therein.

(20) Calderazzo, F.; Pampaloni, G.; Rocchi, L. *J. Organomet. Chem.* **1991**, 413, 91.

(21) Yoon, M.; Lin, J.-H.; Young, V. G.; Miller, G. J. *J. Organomet. Chem.* **1996**, 507, 31.

(22) Deacon, G. B.; Shen, Q. *J. Organomet. Chem.* **1996**, 511, 1.

(23) Protchenko, A. V.; Zakharov, L. N.; Bochkarev, M. N.; Struchkov, Yu. T. *J. Organomet. Chem.* **1993**, 447, 209.

(24) Roitershtein, D. M.; Rybakova, L. F.; Petrov, E. S.; Ellern, A. M.; Antipin, M. Yu.; Struchkov, Yu. T. *J. Organomet. Chem.* **1993**, 460, 39.

(25) Hogerheide, M. P.; Boersma, J.; Spek, A. L.; van Koten, G. *Organometallics* **1996**, 15, 1505.

(26) Hazin, P. N.; Bruno, J. W.; Schulte, G. K. *Organometallics* **1990**, 9, 416.

(27) Stults, S. D.; Andersen, R. A.; Zalkin, A. *Organometallics* **1990**, 9, 115.

Table 4. X-Band EPR Spectral Temperature-Dependent Parameters of the A–D La(II) Paramagnetic Species

species	g_{\parallel}^a	g_{\perp}^a	$\langle g \rangle$	g_{iso}^b	a_{\parallel}^a	a_{\perp}^a	$\langle a \rangle$	a_{iso}^b
A	2.028	1.979	1.995	1.988	137.3	145.3	142.6	146.2
B	2.017	1.968 ^c	1.984 ^c	1.975	121.0	≥ 121.1 ^c	≥ 136.1 ^c	136.1
C				1.994				147.1
D				≥ 1.994				≥ 147.1

^a $T = 100$ K. ^b $T = 280$ K. $g_i = 6 \times 10^{-3}$; $a_i = 6 \times 10^{-1}$ G; $\langle g_i \rangle = 1/3(g_{\parallel} + 2g_{\perp})$; $\langle a_i \rangle = 1/3(a_{\parallel} + 2a_{\perp})$. ^c Computed values.

The two more intense absorptions (hereafter **A**, the most intense, and **B**, the less intense, lanthanum(II) paramagnetic species) exhibited isotropic line shapes of well-separated octuplets, overlapping in the center field region. The heights of the lines of each multiplet decreased upon increasing the applied magnetic field H , while, correspondingly, the actual line widths progressively increased from lower to higher field, together with the relevant peak-to-peak separation. The third less intense absorption **C** is attributed to a third lanthanum(II) species and was EPR-detectable only for the first five lines of its overall absorption pattern [as particularly evident from the second derivative mode (Figure 4b), where the individual m_l -lines of the most intense **A** lanthanum(II) species were differently affected by the corresponding m_l -lines of the **C** lanthanum(II) species, which progressively overlapped the **A** later ones]. The fourth absorption set **D** (the least intense) was detectable only for the first low-field absorption line, the other higher field lines being totally overlapped by the most intense **A–C** spectral features. As far as the actual signal is concerned, the relevant field position excludes any “free radical” (organic in nature) character. For the **A–D** multiplets, the fluid solution EPR computed line shape indicates that the actual g_{iso} values are typical of paramagnetic species displaying significant metal character.²⁹ Accordingly, each of the four absorption sets exhibited spectral multiplicity arising from the hyperfine coupling of the unpaired electron with the ¹³⁹La nucleus, with $g_{\text{iso}}(\mathbf{A}) = 1.988(6)$, $A_{\text{iso}}(\mathbf{A})(^{139}\text{La}) = 146.8(4)$ G; $g_{\text{iso}}(\mathbf{B}) = 1.975(6)$, $A_{\text{iso}}(\mathbf{B})(^{139}\text{La}) = 136.1(4)$ G (the overall paramagnetic parameters are assembled in Table 4). On the basis of the actual EPR spectral analysis, for all the La(II) species the following features (i)–(iii) are clearly evident. (i) There is a slight but significant broadening of the line shapes as the applied field H_0 increases, as a consequence of the different $m_l^{139}\text{La}$ values. This spectral behavior is typical of strongly metal-centered paramagnetic systems and indicates that the molecular structural anisotropies are not completely averaged.³⁰ (ii) A noticeable second-order contribution to the various A_{iso} coupling constants is evident (i.e., there is an increase in the peak-to-peak hyperfine separation with increasing applied field H_0). Such an effect, particularly evident for magnetically active nuclei with high nuclear spin values I , further supports the metal nature of the actual spectra.^{28,29} (iii) The liquid solution line shapes are very sharp, suggesting that long electron spin relaxation times are experienced by the lanthanum(II) complexes' unpaired electron under fast motion conditions (see the correspondingly much broader liquid

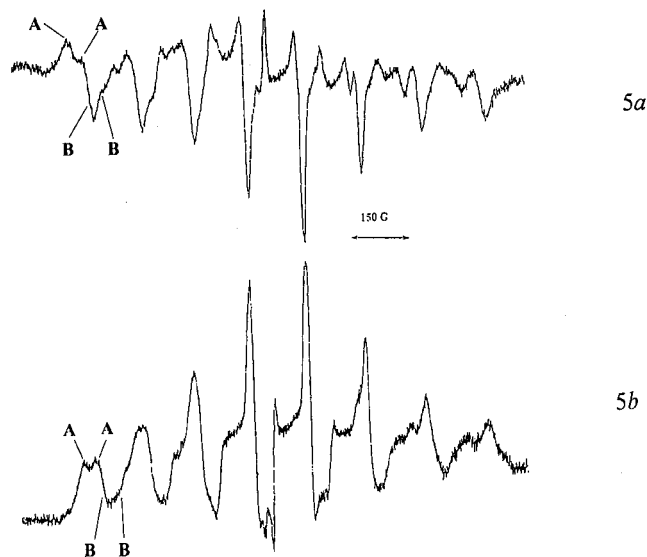


Figure 5. X-Band EPR spectra of the paramagnetic La(II) species **A–D** in (a) first derivative mode and (b) second derivative mode, $T = 100$ K.

nitrogen spectra, discussed below) even in the presence of large lanthanum(II) spin–orbit coupling, reflecting some symmetry of the different molecular frameworks.³⁰ In this picture, a very minor, if any, superhyperfine interaction of the $S = 1/2$ electron with the differently ligated magnetically active nuclei of the four **A–D** lanthanum(II) species is expected. Taking into account the broadest absorption line of the actual octuplets (i.e., that corresponding to $m_l = -7/2$), an upper limit for such an interaction can be proposed: $\Delta H_{m_l=-7/2} > A_{\text{iso}}(^1\text{H})$.

Figure 5 (5a first derivative mode; 5b second derivative mode) shows the corresponding spectra at liquid nitrogen ($T = 100$ K) temperature, displaying broad and partially resolved anisotropic signals which overlapped in the medium-field region.

In this case the computed line shape analysis allows us to directly detect only two of the previous isotropic signals (the most intense **A** and **B** signals), both displaying poorly separated axial structure, as follows: $g_{\parallel}(\mathbf{A}, \mathbf{B}) > g_{\perp}(\mathbf{A}, \mathbf{B}) \neq g_{\text{electron}}$. On the other hand, the minor **C** and **D** absorption patterns were totally overlapped and undetectable, due to the large experimental anisotropic line widths, which, as verified under the fluid solution conditions, did not allow us to detect any ligand superhyperfine coupling. Moreover, in the overall range of the applied magnetic field H_0 , the glassy spectra displayed ΔH_{axial} dependence in both the parallel and perpendicular spectral regions, as a consequence of active g - and A -strain effects, once more confirming the metal nature of the frozen spectra.³¹

The corresponding computed values are as follows: $g_{\parallel}(\mathbf{A}) = 2.028(6)$, $g_{\perp}(\mathbf{A}) = 1.979(6)$, $\langle g \rangle(\mathbf{A}) = 1.995(6)$; $g_{\parallel}(\mathbf{B}) = 2.017(6)$, $g_{\perp}(\mathbf{B}) = 1.968(6)$, $\langle g \rangle(\mathbf{B}) = 1.984(6)$; $g_{\text{iso}}(\mathbf{C}) = 1.994$; $g_{\text{iso}}(\mathbf{D}) \geq 1.994$.

(31) Mabbs, F. E.; Collison, D. In *Electron Paramagnetic Resonance of d Transition Metal Compounds*; Elsevier: New York, 1992.

(29) Lozos, J. P.; Hoffman, B. M.; Franz, C. G. *QCPE* **1973**, 243. Della Lunga, G. *ESRMR Simulation Program*, University of Siena, 1995.

(30) Kivelson, D.; Neiman, R. *J. Chem. Phys.* **1961**, *35*, 149.

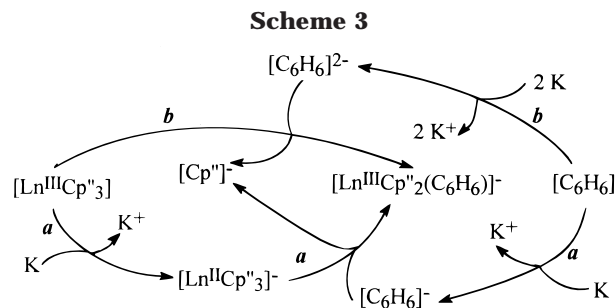
(**B**) = 2.017(6), $g_{\perp}(\mathbf{B}) = 1.968(6)$, $\langle g \rangle(\mathbf{B}) = 1.984(6)$; $\delta g_{\perp, \parallel}(\mathbf{A}, \mathbf{B}) = g_{\parallel}(\mathbf{A}, \mathbf{B}) - g_{\perp}(\mathbf{A}, \mathbf{B}) = 0.048(6)$, $0.049(6)$, respectively.

The relevant liquid nitrogen X-band EPR spectral parameters are listed in Table 4. This emphasizes the significant proximity between the g_{iso} and A_{iso} values and the corresponding $\langle g \rangle$ and $\langle A \rangle$ values of the **A** and **B** species, suggesting the maintenance of the overall geometry of such complex species under very different experimental conditions. On the other hand, it is interesting to note that there is a temperature-dependent variation of the percentage of the **A–D** species under fluid solution conditions. In particular, while at $T = 280$ K the **A–D** La(II) species are detectable with relative spectral intensity **A:B:C:D** = 22:6:5:1, at $T = 297$ K the paramagnetic species reduces to three, **D** being EPR-undetectable, with relative intensity ratios **A:B:C:D** = 26:5:4:0. The different spectral intensities are suitably computed on the basis of the typical relationship $I_i = \text{spectral intensity of the } i\text{th La(II) species} = [(\Delta H_{m_i-7/2})^2 (h_{m_i-7/2})]$, where $\Delta H_{m_i-7/2}$ is the line width of the highest and narrowest line of the actual i th octuplet (here, $m_i = -7/2$) while $h_{m_i-7/2}$ is the corresponding height, the isotropic spectra being recorded under the same experimental and technical conditions.³¹ This spectral behavior is reversible in the actual fluid solution temperature range ($T = 280$ – 297 K) and is consistent with the occurrence of a chemical equilibrium between the various paramagnetic lanthanum(II) species. On the other hand, refreezing to liquid nitrogen temperature the fluid solution almost quantitatively reproduced the previous anisotropic spectra of Figure 5, demonstrating the stability of the different species under varying experimental conditions.

In contrast to our previous observations on a related system,⁸ these spectra showed no evidence of the presence of the benzene radical anion $[\text{C}_6\text{H}_6]^-$. The actual g_{iso} and A_{iso} values, as well as the occurrence of a temperature-dependent equilibrium, are very similar to those found for the paramagnetic metal intermediates involved in the reduction of $[\text{LaCp}''_3]$ with K in DME to give $\{[\text{LaCp}''_2(\mu\text{-OMe})]\}_2$.⁵ Moreover we never observed any relevant line-broadening effect and hyperfine couplings due to the magnetically active ^{41}K nucleus (natural abundance = 6.9%; $I = 3/2$); thus we conclude that K^+ , as a cation, has no influence on the La(II) paramagnetic intermediates. Furthermore, the EPR spectral evidence for the La(II) species, showing very sharp isotropic absorption, supports such a conclusion. The reaction was analyzed by EPR spectroscopy during a 24 h period until the formation of the typical dark red, diamagnetic, EPR-silent, final product **5** was formed.

Bonding in Complexes 5, 6, and 8 and Mechanism of Their Formation. From the experimental data presented in the foregoing sections, we conclude that each of the complexes **5–8** consists of tight ion pairs. Each pair comprises an eight-coordinate potassium-centered cation having six oxygen and two $\eta^2\text{-C}_6\text{H}_6$ contacts, the C_6H_6 moiety acting as a bridging ligand between the potassium and the anionic lanthanoid metalate(III) atoms. The bridge is thus a benzene dianion $[\text{C}_6\text{H}_6]^{2-}$, i.e., a 1,4-cyclohexa-2,5-dienyl ligand.

The assignment of the +3 oxidation state for the lanthanoid metal is inferred from the diamagnetism of



the lanthanate(III) complex **5**, the isostructural relationship of the crystalline complexes **5**, **6**, and **8**, and the spectral similarities between the four complexes $[\text{K}([\text{18-crown-6})][\text{LnCp}''_2(\text{C}_6\text{H}_6)]$ **5–8**. The diene–diyl nature of the C_6H_6 ligand in **5–8** is supported by (i) the crystallographic data for **5**, **6**, and **8**; (ii) the similarity in the metal-to-carbon bonding in a number of transition metal complexes having a substituted arene, naphthalene, or anthracene as coligand; and (iii) their hydrolysis, yielding cyclohexa-1,4-diene.

Complexes **5–8** are the first examples of compounds having a coordinated *unsubstituted* benzene dianion; crystal structures of lithium complexes of naphthalene, anthracene, and fluorene have been reported.³³ The simplest examples of alkali metal complexes of a substituted-benzene dianion relate to the poly(trimethylsilyl) derivatives, $[\text{Li}(\text{THF})]_2[\text{C}_6(\text{SiMe}_3)_6]$ (**9**)³⁴ and $[\text{Li}(\text{DME})]_2[\text{C}_6\text{H}_2(\text{SiMe}_3)_{4-1,2,4,5}]$.³⁵ In crystalline **9**, both lithium atoms lie on the same side of the boat-shaped C_6 ring; the bond lengths to C-1 and C-4 are 1.51 ± 0.02 Å and to the two remaining out-of-plane carbons are 1.39 ± 0.01 Å. The crystalline **10** was described as the first $6\text{C}-8\pi$ antiaromatic benzene dianion, since [as with bis(alkali metal) derivatives of polynuclear fused arenes] the lithium atoms are located above and below the center of the C_6 ring, which is almost planar, having a dihedral angle of only 8° between the $\text{C}(1)-\text{C}(6)-\text{C}(5)$ and $\text{C}(2)-\text{C}(3)-\text{C}(4)$ planes. The C–C bond lengths are nearly equal: 1.415 Å [$\text{C}(2)-\text{C}(3)$], 1.392 Å [$\text{C}(3)-\text{C}(4)$], and 1.413 ± 3 Å for the remaining two. The endocyclic bond angles range from 113.5° to 115.3° at C(1), C(2), C(4), and C(5), but at C(3) and C(6) are 128.9° . There has been much theoretical discussion relating to the structure of the benzene dianion.^{36,37}

Plausible reaction pathways a and b from $[\text{LnCp}''_3]$ (**1–4**) to $[\text{K}([\text{18-crown-6})][\text{LnCp}''_2(\text{C}_6\text{H}_6)]$ (**5–8**) are illustrated in Scheme 3. Thus, we propose that potassium with the crown ether converts benzene to either the benzene anion (pathway a) or the benzene dianion (pathway b). For pathway a, it is necessary to postulate a $\text{Ln(III)} \rightarrow \text{Ln(II)}$ one-electron reduction, and earlier studies had shown that at least two types of Ln(II) intermediates for the case of $\text{Ln} = \text{La}$ can be identified,⁵ these being solvated neutral $[\text{LnCp}''_2(\text{solvent})_n]$ or anionic

(32) Figgis, B. N. In *Introduction to Ligand Fields*; Wiley and Sons: New York, 1966.

(33) For a review, see: Setzer, W. W.; Schleyer, P. v. R. *Adv. Organomet. Chem.* **1985**, *24*, 353.

(34) Sekiguchi, A.; Ebata, K.; Kabuto, C.; Sakurai, H. *J. Am. Chem. Soc.* **1991**, *113*, 1464.

(35) Sekiguchi, A.; Ebata, K.; Kabuto, C.; Sakurai, H. *J. Am. Chem. Soc.* **1991**, *113*, 7081.

(36) Jesse, R. E.; Hoytink, G. J. *Chem. Phys. Lett.* **1967**, *1*, 109.

(37) Nakayama, M.; Ishikawa, H.; Nakano, T.; Kikuchi, O. *J. Mol. Struct. (THEOCHEM)* **1989**, *184*, 369, and references therein.

$[\text{LnCp}''_3(\text{solv})_n]^-$ species; the latter is arbitrarily chosen in our representation in Scheme 3, which in the final step is envisaged to undergo a nucleophilic displacement of $[\text{Cp}''^-]$ by $[\text{C}_6\text{H}_6]^-$ with concomitant $\text{Ln} \rightarrow$ benzene one-electron transfer. The alternative (b) is a nucleophilic substitution of $[\text{Cp}''^-]$ by $[\text{C}_6\text{H}_6]^-$ from the $[\text{LnCp}''_3]$ substrate. Evidence for La(II) species is provided by the EPR spectral data (vide supra).

Conclusions

We have shown that treatment of the tris(cyclopentadienyl)lanthanoid metal(III) complexes $[\text{LnCp}''_3]$ [$\text{Ln} = \text{La}$ (**1**), Ce (**2**), Pr (**3**), or Nd (**4**)] with potassium and ([18]-crown-6) in benzene yields, via paramagnetic La-(II) intermediates, the novel, crystalline complexes $[\text{K}([\text{18}]\text{-crown-6})][\text{LnCp}''_2(\text{C}_6\text{H}_6)]$ **5–8**, respectively, which are formulated as containing lanthanate(III) anions having not only two $[\text{Cp}''^-]$ but also a 1,4-cyclohexa-3,5-dienyl ligand, the latter also acting as a bridge between the potassium and the Ln metal atom. These complexes

are the first examples of such a ligated unsubstituted benzene dianion. Their hydrolysis yields cyclohexa-1,4-diene, its formation from benzene thus being a Birch-type reduction. Complexes **5–8** are probably forerunners of a larger group of metal complexes that are expected to show unusual reactivity.

Acknowledgment. We thank the European Community (Marie Curie fellowship for M.C.C.) and EPSRC for the award of a fellowship for Y.K.G. and for other support.

Supporting Information Available: Details about the crystal structures; including ORTEP diagrams, and tables of crystal data and structure refinement, atomic coordinates, bond lengths and angles, and anisotropic displacement parameters for **5**, **6**, and **8**; and computer-simulated EPR spectra relating to the **A** and **B** species of Figure 4a,b. This material is available free of charge via the Internet at <http://pubs.acs.org>.

OM990536X